

Marine CSEM time-lapse repeatability for hydrocarbon field monitoring

J.J. Zach (jjz@emgs.com), M.A. Frenkel (maf@emgs.com), D. Ridyard (dr@emgs.com), J. Hincapie (jhincapie@emgs.com), B. Dubois (bdubois@emgs.com), J.P. Morten (jpmorten@emgs.com): EMGS

Summary

The marine Controlled-Source Electromagnetic (CSEM) method has become a well-established geophysical tool for 3D imaging of multiple resistive bodies. While traditionally being considered an exploration tool, improved data quality and advanced processing methods put mapping detailed resistivity distributions using CSEM methods in reach. Particularly in conjunction with 3D- and 4D-seismic technology defining the structural container, marine CSEM can add a complementary image of the bulk distribution of resistors. Using real data and supported by modeling, we assess the capability of CSEM technology for time-lapse monitoring, including the dominant sources of non-repeatability.

Introduction

Commercial hydrocarbon exploration using marine controlled-source electromagnetic (CSEM) methods using ocean bottom receivers and a ship-towed bipole have been used since 2002 (Eidesmo et al., 2002) and have experienced rapid growth in technology and market penetration. The principal detection mechanism is the relative enhancement of the transverse magnetic component of the received electromagnetic signal by resistors buried in the subsurface. These resistors can be either hydrocarbon deposits or other resistive bodies. The source emits a periodic signal consisting of a number of discrete frequencies which form the basis for survey design, processing and data inversion.

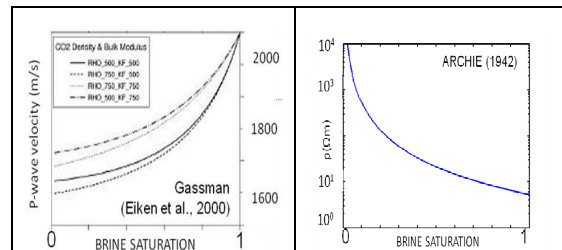
A vast improvement in data quality over the past years was driven by advances in hardware and operations, permitting the acquisition of well-defined and repeatable grids of seabed receivers with complex towing patterns including the acquisition of wide-azimuth data. Together with advances in inversion and integrating CSEM data into global geophysical interpretations (Buonora et al., 2008), marine CSEM has become an established method for 3D imaging of complex geological settings. For references, see the case studies presented in Carrazone et al., 2008, Price et al., 2008, Plessix, van der Sman, 2008 and Zach and Frenkel, 2009.

While depth migration of CSEM data has been demonstrated in simple cases (Mittet et al., 2005), all commercially viable solutions for 3D imaging of the subsurface rely on a gradient-based, iterative inversion approach in which the full set of Maxwell's equations is solved on a finite grid during each iteration step. The model

change after each step is determined from the gradient $g = \partial \varepsilon / \partial \sigma_i$ of a misfit functional ε with respect to the conductivities in a discretized model σ_i . Approaches such as presented in Zach et al., 2008-1 and 2009 constitute a full-waveform inversion, which is more robust in CSEM compared to the seismic case on account of the lower resolution due to the diffusive nature of the wave-field compared to the latter. Among the notable recent publications on full-waveform marine CSEM 3D inversion are for example Commer et al., 2008, Jing et al., 2008, Gribenko and Zhdanov, 2007.

There is considerable added value in joint interpretation of CSEM and seismic surveys. The complementary relation between the methods has two major aspects:

- (1) Seismic techniques are sensitive to structural boundaries, whereas CSEM anomalies depend on the existence of a sufficient contrast in transverse resistance $R_t = (\Delta \rho)(\Delta z)$ and are thus sensitive to the bulk volume of a resistor (hydrocarbons or other); it is important to note that Δz can be considerably smaller than the inherent resolution of the method to generate a response.
- (2) CSEM responds to resistivity, which tends to be sensitive to changes between high to intermediate hydrocarbon saturation, as opposed to seismic attributes such as the p-wave velocity, which is flat in the same saturation range. Conversely, CSEM has little sensitivity to



fizz gas compared to 3D seismic techniques (see figure 1).

Figure 1: LEFT: Seismic p-wave velocity versus the brine saturation (Eiken et al., 2000). RIGHT: Resistivity versus brine saturation following Archie (1942).

While joint inversion in the narrow sense is of considerable academic interest (e.g., Hoversten et al., 2006), present-day applications focus either on joint interpretation of 3D seismic images and resistivity cubes from 3D-CSEM inversion, or on using seismic containers to constrain CSEM-inversion.

In the present case study, the inversion result from a dense 3D CSEM grid acquired over an area with high-quality 3D

Marine CSEM time-lapse repeatability for hydrocarbon field monitoring

seismic data is discussed. The next logical step beyond 3D-CSEM surveys are time-lapse-, or 4D-CSEM surveys, and have the greatest potential when jointly acquired with time-lapse seismic data. At this point, published time-lapse CSEM surveys are at the stage of detailed survey planning (e.g., Norman et al., 2008, Lien and Mannseth, 2008). In the present contribution, we will evaluate the time-lapse capability of the acquisition mode at the time of publication, and discuss the first two among the following possible sources of non-repeatability:

- (1) Source navigation and waveform,
- (2) Ocean bottom receiver position and orientation,
- (3) Cultural changes between repeat acquisitions (e.g., additional subsea installations).

Methodology 1: Data acquisition and conditioning

Source-receiver synchronization

Marine CSEM data consist of time-series data acquired by ocean bottom receivers, which are arranged in grids or lines. Horizontal electric and magnetic fields (4-component), and optional vertical fields, are recorded every 20ms, as a horizontal bipole is towed <100m above the seafloor, see figure 2. Since the receivers operate autonomously between drop and retrieval, their clocks have to be synchronized to the source, which is accurate to better than 10ms over several days. In order to achieve this accuracy, a temperature-dependent correction is applied to the clock calibration. For a typical 0.25 Hz- mode, this is equivalent to a phase error between source and receiver of better than 1 degree. This implies controlled amplitude and phase throughout receiver grids outlined in figure 3, which is essential to achieve depth sensitivity in inversion. Source navigation data are measured including position and orientation of the source, using a suite of acoustic and echo-sounder sensors on the vessel and the source. However, source navigation accuracy depends on water depth, but is generally given to within ~meters in the horizontal position, ~10 cm in vertical altitude above the seafloor and less than 1 degree for the source dipole orientation. Navigation data are recorded every 10 seconds, and an interpolation method is used to assign a source position to each electric field measurement.

Data conditioning for advanced processing

The data conditioning follows the approach outlined in Zach et al., 2008-2, where data are converted into the frequency domain and the data noise is obtained, which is essential for weight generation in subsequent inversion. The receiver angle is determined with a proprietary data-driven method similar to the one described in Mittet et al., 2007. It should be stated that no subsequent timing/phase corrections are necessary at the state of the art.

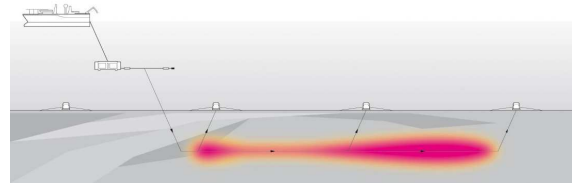


Figure 2: Marine CSEM acquisition mode: a horizontal bipole (~300m), which is towed ~30m above the seafloor emits a periodic current pulse with a peak of up to a few thousand Amperes and a frequency spectrum in the range 0.01-15Hz. Data are comprised by 4- or 6-component electric and magnetic fields recorded at seabed stations arranged in grids with any complexity.

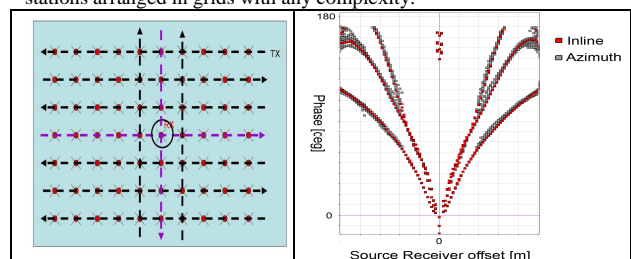


Figure 3: Left: typical grid of receivers with data being recorded for each receiver for both inline (purple) and azimuth (black) lines. Right: Full phase control is demonstrated by plotting the phase one receiver and the 0.25 Hz- and 0.75 Hz-modes for inline and azimuthal data; example from the Norwegian Sea, 2008.

Methodology 2: 3D inversion of marine CSEM data

The 3D inversion methodology applied here is based on Zach et al., 2008-1 and 2009. The gradient calculation in the iterative inversion loop is based on the first Born-scattering assumption of the relationship between model- and field-perturbation (Støren et al., 2008). A fast finite-difference time-domain solver based on Maaø, 2007 was used to generate synthetic data. The optimization is based on a quasi-Newton update using the known gradient and an approximate calculation of the inverse Hessian matrix.

Example from offshore Norway

A 3D CSEM grid survey with 1.25 km grid spacing, consisting of 54 receivers, was acquired in the Norwegian North Sea in March 2008. The source waveform was mainly a triple peak with the modes 0.25, 0.75 and 1.25 Hz, with approximately equal amplitudes. The target is the Troll oil province, a few km west of the Troll West gas field, which is a well-known CSEM calibration target. The starting model used was based on measured bathymetry and plane-layer inversion of a reference receiver following Roth and Zach, 2007. An image of the final resistivity cube is shown in figure 4, which confirms the strong anomaly due to the gas field, the known geology of the area and an outline of the resistive response within the boundaries of the seismic prospect of the Troll oil field. In general, within the resolution of the CSEM method, proven well logs

Marine CSEM time-lapse repeatability for hydrocarbon field monitoring

throughout the area are confirmed. Most importantly, the resistivity distribution within the reservoir is visible, for example the gas cap on top of the oil reservoir.

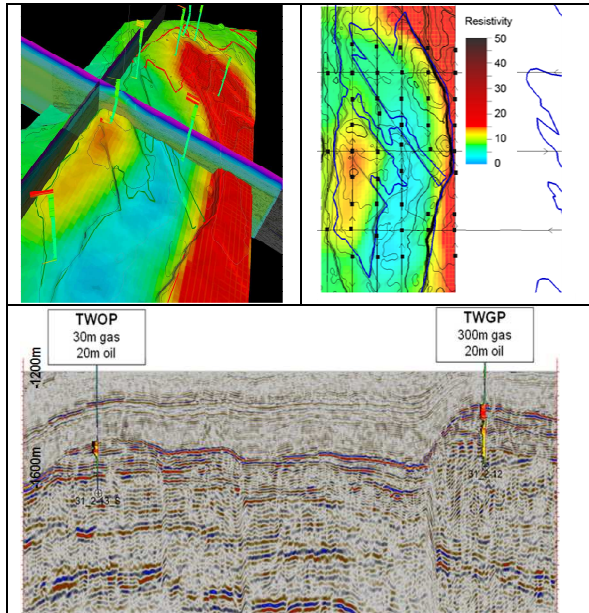


Figure 4: Final inversion result for 3D inversion of electric data including both inline and azimuthal fields from a 3D grid over the Troll oil province. Top panel: Resistivity in inversion cube draped onto prospect level; bottom panel: seismic section through two principal wells in both the Troll oil- and Troll West gas province.

The next step: time-lapse CSEM

In past surveys, the greatest acquisition uncertainty related to the receiver orientation, which introduced a systematic error of up 3-5 degrees in azimuth and tilt. With more accurate receiver orientation measurements and the possibility to use seabed monuments, future sources of non-repeatability for time-lapse surveys will be dominated by the source navigation. Table 1 lists the present versus future contributions of the most relevant source parameters to the time-lapse error. The cumulative error based on source navigation only from a recent dataset in the Gulf of Mexico, where part of a survey was towed twice over the same receiver drop, is shown in figure 5, where the resulting time-lapse repeatability is within 3-5%.

Time-lapse feasibility modeling

One of the key potential 4D-CSEM applications is time-lapse waterflood monitoring in hydrocarbon reservoirs, particularly to distinguish different shapes of the advancing waterfront. Figure 6 shows a numerical experiment with a 10km x 10km reservoir, one fifth of which is flooded from the left. In both cases, the volume of the flood is the same, but the shape is different, representing compartmentalized

reservoirs. As time-lapse responses, we consider the measured field after versus before flooding, which are plotted for three receiver lines in figure 7. Only the Eastern electric field component is plotted, and only responses are plotted for which the received signal is at least one order of magnitude above the noise threshold (assumed to be $10^{-15} \text{V}/\text{Am}^2$). The flood causes a 30%-50% anomaly level, whereas different realistic flooding patterns can distinguish each other on a 10% anomaly level. With a 5% repeatability error in time-lapse surveys established with today's marine CSEM technology, we therefore conclude that in large reservoirs, both production and water flood as such, as well as different shapes of water flood can be monitored.

Table 1: Major sources of time-lapse source non-repeatability.

Parameter	Present -day receiver data error	Mitigate effect on time-lapse with present-day technology	Further mitigation with moderate technology upgrade
	<2% for $\Delta=5\text{m}$	Corrections based on modeling or re-datuming possible; fully implemented in inversion. Aim for survey plan in flat bathymetry.	Improve with better source position information & navigation: ~1-3m accuracy expected.
	<3% f. 5 dgr.	Modeling-based correction possible; fully implemented in inversion. Aim for flat bathymetry where possible.	Improve with better source position information & navigation: within 1 dgr. Parallel to seafloor expected.
	<1% for $\Delta<50\text{m}$	Minor problem due to accurate receiver positioning; fully implemented in inversion.	Better receiver positioning, source navigation. Acquisition standards approach 10m.
	1-5% for 10 degrees	Modeling-based correction possible; fully implemented in inversion. Attempt repeating survey in similar ocean current conditions.	Better source navigation, actively steered source.

Marine CSEM time-lapse repeatability for hydrocarbon field monitoring

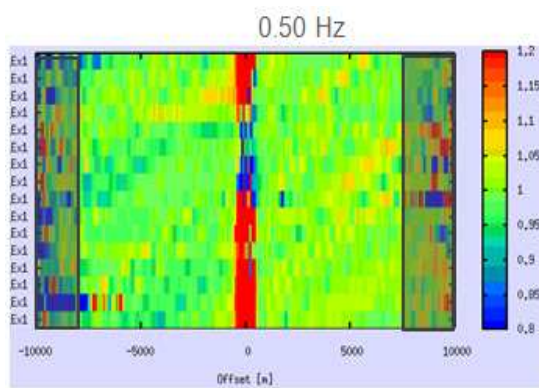


Figure 5: Time-lapse repeatability: relative magnitude versus offset of inline electric data, whereby subsequent tows were normalized against each other.

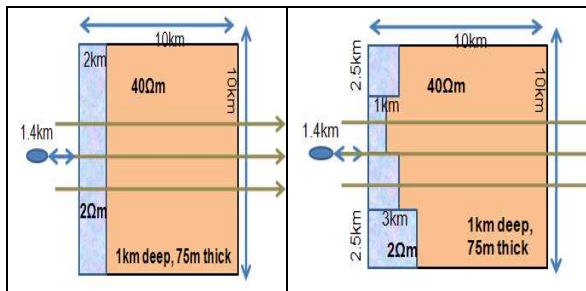


Figure 6: Top view of reservoir model with two different shapes of identical volume water floods. The source bipole is located 6.4km to the left of the reservoir edge, and the received signal is compared along the three olive-green lines shown.

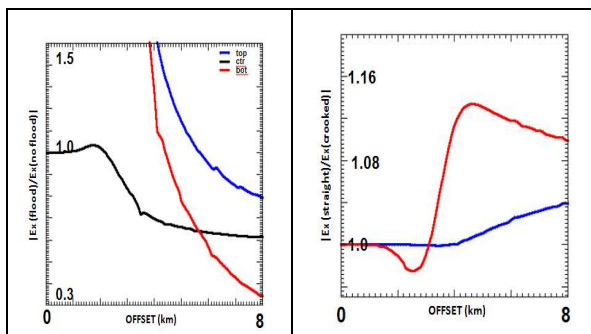


Figure 7: Time-lapse signal for the water flood shown in figure 11. Top: for $f=0.25$ Hz, the Eastern electric field after versus before the flood for the three lines shown in the right panel of figure 6. The anomaly is detectable on a 30%-50% anomaly level. Bottom: the Eastern electric field of the "crooked" flood on the right versus the "straight" flood on the left panel of figure 6. The relative difference in the signal between both flood shapes is therefore detectable, if a time-lapse error of ~5% is assumed. Color legend: blue: top line, red: bottom line, black: center line in fig. 6.

Finally, figure 8 shows the relative time-lapse signal of a partial water flood, showing a 20%-anomaly, even if the resistivity only decreases by 50%, also resolvable using state of the art-CSEM surveys.

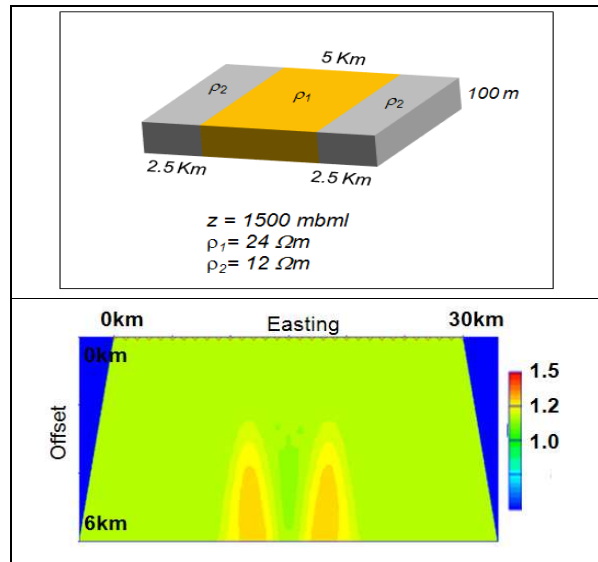


Figure 8: Water flood (grey) in a hydrocarbon reservoir (orange) at 1.5 km below sea level. Top: schematic of the reservoir. Bottom: normalized time-lapse signal of produced versus unproduced reservoir (CMP-line summary plot over CSEM receiver line over center of reservoir).

Conclusions

The present inversion-based 3D interpretation approach is, together with constraints from seismic and/or well data, able to quantitatively map resistivity within larger reservoirs. Time-lapse surveys for production- and water flood monitoring, including distinguishing different flood shapes, are feasible for the present state of the art of acquisition technology. Time-lapse repeatability due to the source alone is in the sub-5%-range, and is set to drop further for improved navigation, as well as improved advanced processing which takes into account the existing accurate navigation measurements.

Acknowledgements

We thank StatoilHydro for the right to present the data and results of the 3D acquisition of the Troll oil province, and EMGS for supporting this contribution. Particularly, we thank Anne-Marit Ostvedt-Ghazi and Honglin Yuan (EMGS) for their support for geological modeling.

EDITED REFERENCES

Note: This reference list is a copy-edited version of the reference list submitted by the author. Reference lists for the 2009 SEG Technical Program Expanded Abstracts have been copy edited so that references provided with the online metadata for each paper will achieve a high degree of linking to cited sources that appear on the Web.

REFERENCES

None